Exotic structure and decay of medium mass nuclei near the drip lines within beyond-mean-field approach

A. PETROVICI

Horia Hulubei National Institute for Physics and Nuclear Engineering, Bucharest, Romania

Outline

- ***complex*** **EXCITED VAMPIR** beyond-mean-field model

· ***proton-rich A~70 nuclei***

- shape coexistence, shape transition, pairing correlations

- isospin symmetry breaking effects on Coulomb Energy Differences and competing

superallowed Fermi and Gamow-Teller β-decay

· ***neutron-rich A~100 nuclei***

- triple shape coexistence and shape evolution in the N=58 Sr and Zr isotopes

- Gamow-Teller β-decay relevant for :

- reactor decay heat (^{102,104}Tc)

- r-process (^{104,106}Zr)

Characteristic features of proton-rich A~70 and neutron-rich A~100 nuclei

- ***shape transition, shape coexistence, shape mixing***
- ***drastic changes in structure with isospin, spin, excitation energy***

Open problems for theoretical models

- ***unitary description of evolution in structure at low and high spins***
- ***unitary treatment of structure and β-decay properties***

complex VAMPIR model family

- **the model space is defined by a finite dimensional set of spherical single particle states**

- **the effective many-body Hamiltonian is represented as a sum of one- and two-body terms**

- **the basic building blocks are Hartree-Fock-Bogoliubov (HFB) vacua**

- **the HFB transformations are essentially *complex* and allow for proton-neutron, parity and angular momentum mixing being restricted by time-reversal and axial symmetry**

- **the broken symmetries (s=N, Z, I, p) are restored by projection before variation**

** The models allow to use rather large model spaces and realistic effective interactions*

Beyond-mean-field variational procedure: complex EXCITED VAMPIR model

Vampir

$$E^s[F_1^s] = \frac{\langle F_1^s|\hat{H}\hat{\Theta}_{00}^s|F_1^s\rangle}{\langle F_1^s|\hat{\Theta}_{00}^s|F_1^s\rangle}$$

$\hat{\Theta}^s_{00}$ - *symmetry projector*

$|F^s_1>$ - ***HFB vacuum***

$$|\psi(F_1^s); sM\rangle = \frac{\hat{\Theta}_{M0}^s|F_1^s\rangle}{\sqrt{\langle F_1^s|\hat{\Theta}_{00}^s|F_1^s\rangle}}$$

Excited Vampir

$$|\psi(F_i^s); sM\rangle = \Sigma_{j=1}^{i}|\phi(F_j^s)\rangle\,\alpha_j^i \qquad \text{for} \quad i = 1, ..., n-1$$

$$|\phi(F_i^s); sM\rangle = \hat{\Theta}_{M0}^s|F_i^s\rangle$$

$$|\psi(F_n^s); sM\rangle = \Sigma_{j=1}^{n-1}|\phi(F_j^s)\rangle\,\alpha_j^n + |\phi(F_n^s)\rangle\,\alpha_n^n$$

$$(H - E^{(n)}N)f^n = 0$$

$$(f^{(n)})^+ N f^{(n)} = 1$$

$$|\Psi_\alpha^{(n)}; sM> = \sum_{i=1}^{n}|\psi_i; sM> f_{i\alpha}^{(n)}, \qquad \alpha = 1, \ldots, n$$

A~70 mass *region*

^{40}Ca - core

model space for both: protons and neutrons

$1p_{1/2}$ $1p_{3/2}$ $0f_{5/2}$ $0f_{7/2}$ $1d_{5/2}$ $0g_{9/2}$

(charge-symmetric basis + Coulomb contributions to the π-spe from the core)

A~100 mass *region*

^{40}Ca - core

model space for both protons and neutrons

$1p_{1/2}$ $1p_{3/2}$ $0f_{5/2}$ $0f_{7/2}$ $2s_{1/2}$ $1d_{3/2}$ $1d_{5/2}$ $0g_{7/2}$ $0g_{9/2}$ $0h_{11/2}$

(single-particle energies adjusted within complex MONSTER (VAMPIR))

renormalized G-matrix (OBEP, Bonn A)

- ***pairing properties enhanced by short range Gaussians for:***

  T = 1 pp, np, nn channels

  T = 0, S = 0 and S = 1 channels

- ***onset of deformation influenced by monopole shifts:***

  $\langle 0g_{9/2}\, 0f;\, T=0\, |G|\, 0g_{9/2}\, 0f; T=0 \rangle$

- ***Coulomb interaction between valence protons added***

Isospin symmetry breaking effects

Coulomb Energy Differences

A= 66,70, 82, 86

Exotic case : A = 70

G. de Angelis et al, Eur. Phys. J. A12 (2001) 51 (^{70}Br)

A. M. Hurst et al, Phys. Rev. Lett.98 (2007) 072501
(^{70}Se: No evidence for oblate shapes)

J. Ljungvall et al, Phys. Rev. Lett. 100 (2008) 102502
(^{70}Se: Evidence for oblate shapes)

complex* Excited Vampir: *isospin-symmetry breaking and shape mixing

A. Petrovici, J. Phys.G: Nucl. Part. Phys. 37 (2010) 064036

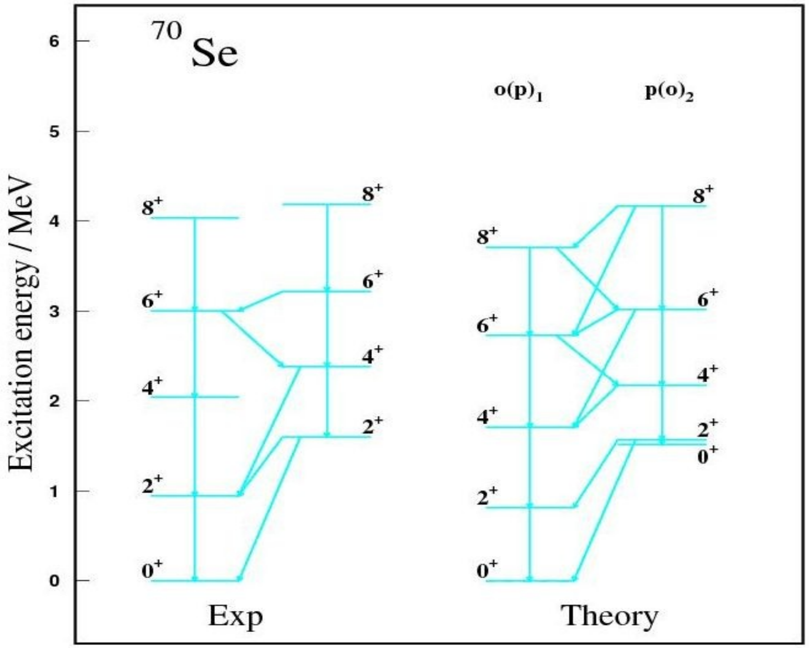

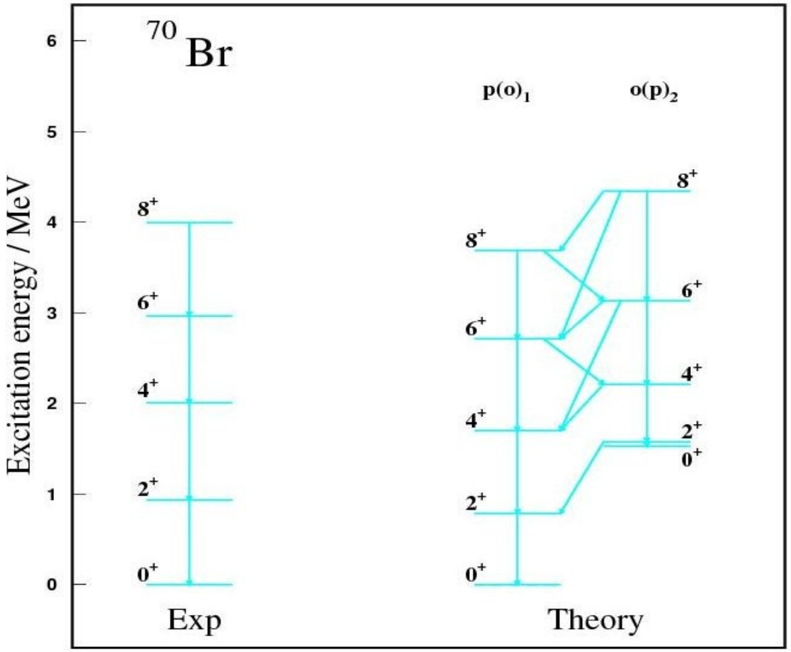

***complex* Excited Vampir results: oblate-prolate mixing specific for each nucleus varying with increasing spin**

Shape mixing manifested in the structure of the wave functions

The amount of mixing for the lowest states in ^{70}Se.

$I[\hbar]$	o-mixing	p-mixing
0_1^+	55%	39%
0_2^+	39%	54%
0_3^+		87%
2_1^+	57%	39%
2_2^+	41%	58%
2_3^+		92%
4_1^+	62%	35%
4_2^+	37%	63%
4_3^+		80(13)%
6_1^+	37%	59%
6_2^+	61%	37%
6_3^+	43%	43%
8_1^+		91%
8_2^+	93%	
8_3^+		84(10)%

The amount of mixing for the lowest states in ^{70}Br.

$I[\hbar]$	o-mixing	p-mixing
0_1^+	35%	62%
0_2^+	59%	34%
0_3^+		88%
2_1^+	41%	57%
2_2^+	58%	40%
2_3^+		94%
4_1^+	41%	56%
4_2^+	57%	41%
4_3^+		94%
6_1^+	20%	76%
6_2^+	79%	20%
6_3^+		44(34)(12)%
8_1^+		89%
8_2^+	96%	
8_3^+		71(11)(11)%

Strong oblate-prolate mixing up to 6^+ : oblate components dominate the yrast states of ^{70}Se, but the yrare states of ^{70}Br

Shape mixing revealed by the spectroscopic quadrupole moments

Spectroscopic Q_2^{sp} (in efm^2) of the lowest three states of spin I of ^{70}Se (effective charges $e_p = 1.2$, $e_n = 0.2$).

$I[\hbar]$	I_1	I_2	I_3
2^+	4.5	-7.	-43.7
4^+	11.5	-16.8	-54.4
6^+	-17.5	9.5	-54.2
8^+	-64.	52.1	-60.

Spectroscopic Q_2^{sp} (in efm^2) of the lowest three states of spin I of ^{70}Br (effective charges $e_p = 1.2$, $e_n = 0.2$).

$I[\hbar]$	I_1	I_2	I_3
2^+	-6.4	4.6	-44.6
4^+	-9.8	5.2	-60.8
6^+	-39.7	33.7	-62.2
8^+	-65.5	59.	-71.4

Precise quadrupole moments for low spin states could clarify the open problem

Shape mixing revealed by the B(E2;ΔI = 2) strengths

$B(E2; I \rightarrow I-2)$ values (in e^2fm^4) for the lowest two bands of ^{70}Se (EXVAM). Strengths for secondary branches are given in parentheses (effective charges $e_p = 1.2$, $e_n = 0.2$) .

$I[\hbar]$	EXVAM $o(p)_1$	$p(o)_2$	Exp.	(HFB-based-config.mix.) (Girod et al.)
2^+	492	501 (5)	342 ± 19	549
4^+	713	761	370 ± 24	955
6^+	779 (62)	792 (33)	530 ± 96	1404
8^+	717 (193)	666 (150)		

$B(E2; I \rightarrow I-2)$ values (in e^2fm^4) for the lowest two bands of ^{70}Br (EXVAM). Strengths for secondary branches are given in parentheses (effective charges $e_p = 1.2$, $e_n = 0.2$).

$I[\hbar]$	$p(o)_1$	$o(p)_2$
2^+	541	516
4^+	775	756
6^+	820 (60)	777 (44)
8^+	771 (81)	754 (84)

A = 82, 86 *analogs*

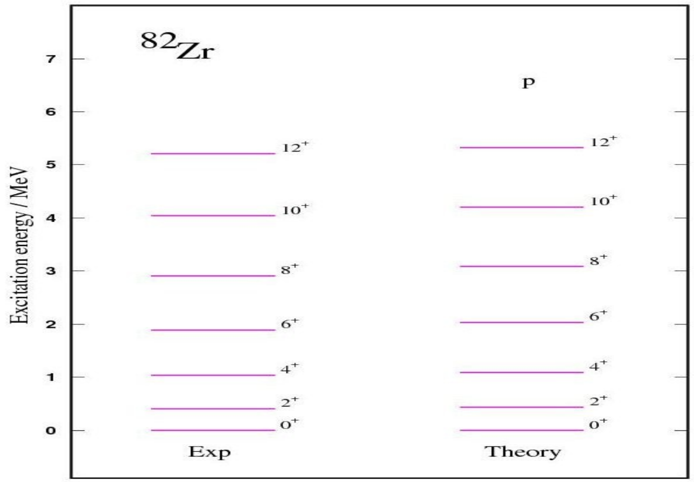

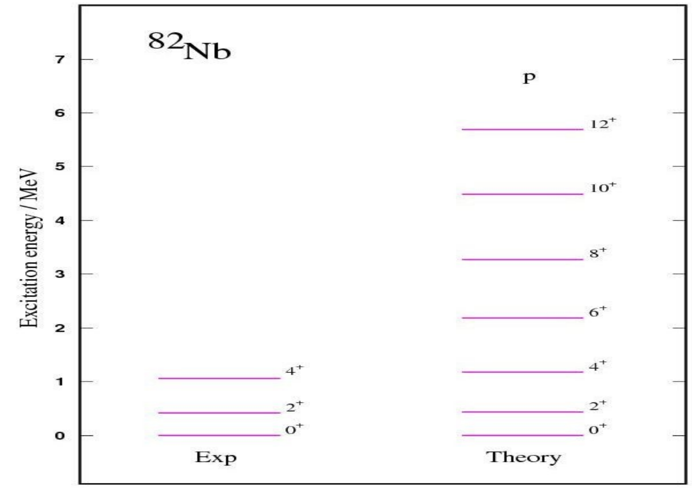

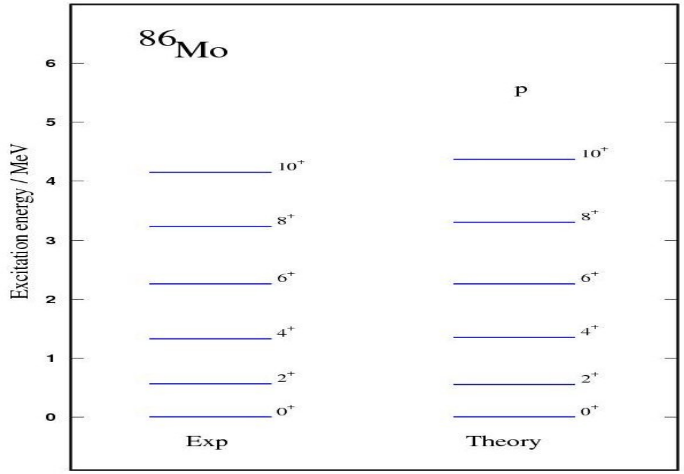

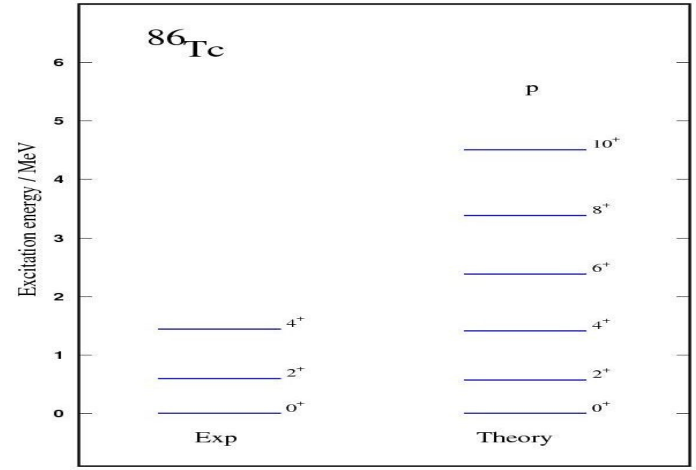

one prolate deformed configuration dominates (>90%) the structure of the yrast states

A. Petrovici et al., Phys. Rev. C78 (2008) 064311

New exotic case: A = 66

$^{66}As - ^{66}Ge$ → *G. de Angelis, A. Petrovici et al., Phys. Rev. C85 (2012) 034320*

complex* Excited Vampir results:** ***different shape mixing changing with spin

The amount of mixing of the lowest states in ^{66}Ge.

$I[\hbar]$	o-mixing	p-mixing ($\mathbf{p}_s$)
0_1^+	18(2)%	77(**2**)(1)%
0_2^+	4%	**82**(10)(4)%
2_1^+	38%	59(2)%
2_2^+	57%	37(6)%
4_1^+	32%	65(1)%
4_2^+	63%	33(3)%
6_1^+	9%	90(1)%
6_2^+	82%	9(5)(3)%

The amount of mixing of the lowest states in ^{66}As.

$I[\hbar]$	o-mixing	p-mixing ($\mathbf{p}_s$)
0_1^+	15(1)%	80(**2**)(2)%
0_2^+	2(2)%	**76**(12)(7)(1)%
2_1^+	29%	68(2)%
2_2^+	64%	31(3)(1)(1)%
4_1^+	18%	80(1)%
4_2^+	76%	18(5)(1)%
6_1^+	4%	95(1)%
6_2^+	81%	14(4)%

Significant oblate-prolate mixing up to 6^+: prolate components dominate the yrast states of ^{66}Ge and ^{66}As

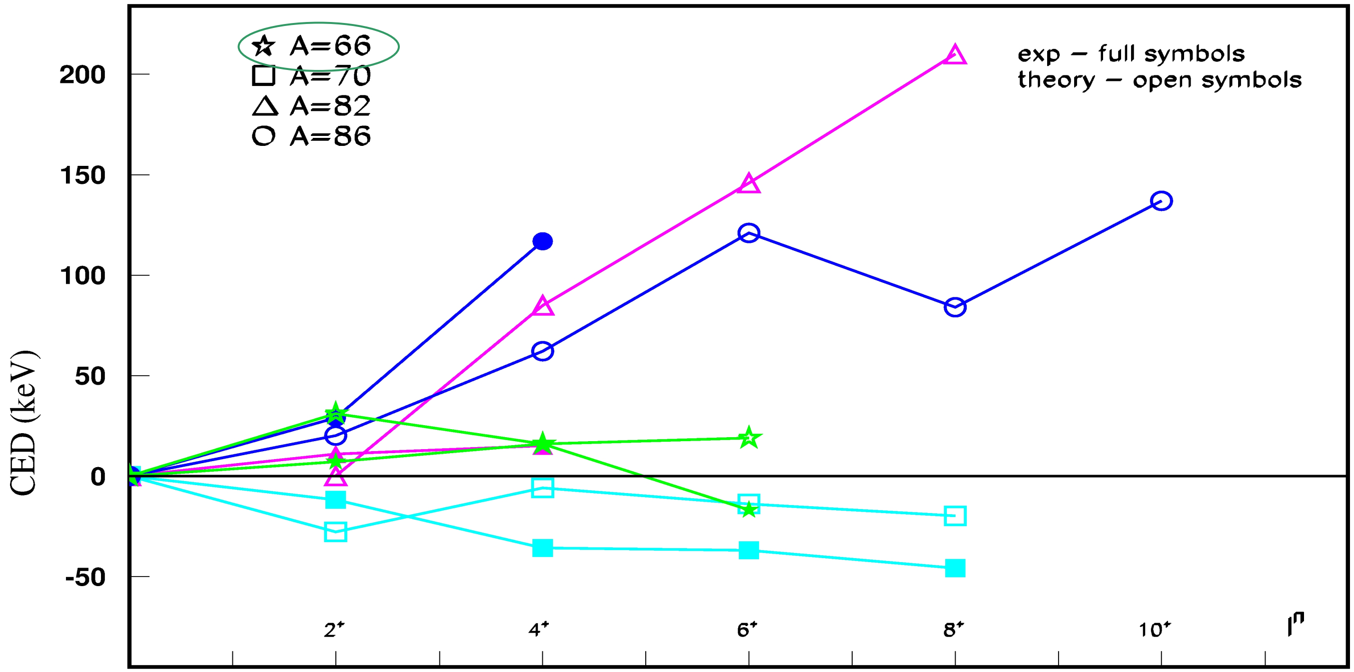

A. Petrovici, J. Phys.G: Nucl. Part. Phys 37 (2010) 064036

* *G. de Angelis, A. Petrovici et al., Phys. Rev. C85 (2012) 034320*

Superallowed β-decays within A=70 isospin vector triplet and pn-pairing correlations

$^{70}Kr \rightarrow {}^{70}Br \rightarrow {}^{70}Se$ superallowed Fermi β-decay — *A. Petrovici et al., Nucl. Phys. A747 (2005) 44*

$^{70}Kr \rightarrow {}^{70}Br$ competing superallowed Fermi and Gamow-Teller β-decay — *Iachello, Padova, 1994*

Accepted experimental proposal, RIKEN, 2013

complex EXCITED VAMPIR predictions

^{70}Kr

$0^+_I \rightarrow$ 49% oblate / 51% prolate

$0^+_{II} \rightarrow$ 44% oblate / 56% prolate

$0^+_{III} \rightarrow$ 14% oblate / 86% prolate

^{70}Br - lowest 1+ states (1.9 MeV, 2.6 MeV, 2.9 MeV)

one dominant EXVAM configuration

$1^+_I \rightarrow$ oblate $1^+_{II} \rightarrow$ prolate $1^+_{III} \rightarrow$ prolate

*B(GT) : $0^+_{gs} \rightarrow 1^+_I$ (**negligible**) / 1^+_{II} (**0.24 $g^2_A/4\pi$**) / 1^+_{III} (**0.16 $g^2_A/4\pi$**)*

Pair structure analysis

pair number operator

$$\rho^{JTT_z\pi}_{(M)} \equiv \frac{1}{2} \sum_{n_il_ij_in_kl_kj_k} \delta((-)^{l_i+l_k}, \pi)(-)^{j_i+j_k-M}(-)^{1-T_z}$$

$$\times \sum_{m_im_k\tau_i\tau_k} \langle j_im_ij_km_k|JM\rangle\langle\frac{1}{2}\tau_i\frac{1}{2}\tau_k|TT_z\rangle c^\dagger_{n_il_ij_im_i\tau_i} c^\dagger_{n_kl_kj_km_k\tau_k}$$

$$\times \sum_{m_rm_s} \langle j_k - m_r j_i - m_s|J - M\rangle\langle\frac{1}{2} - \tau_k\frac{1}{2} - \tau_i|T - T_z\rangle c_{n_kl_kj_km_r\tau_k} c_{n_il_ij_im_s\tau_i}$$

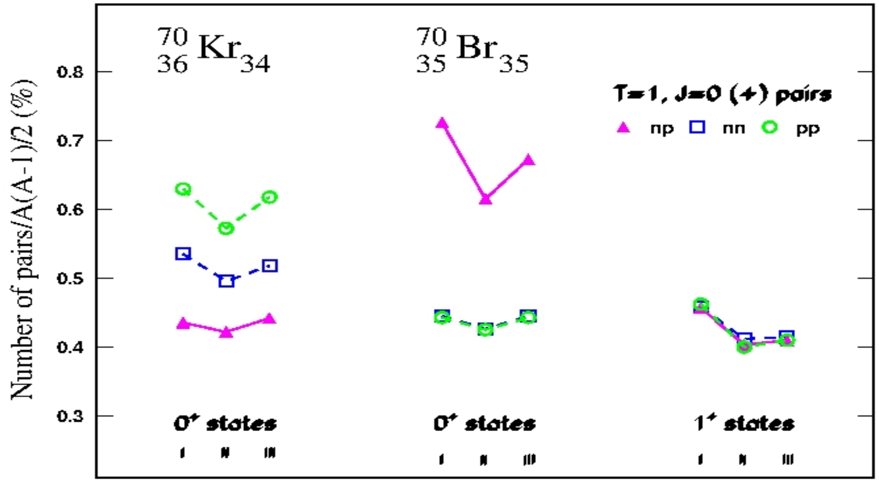

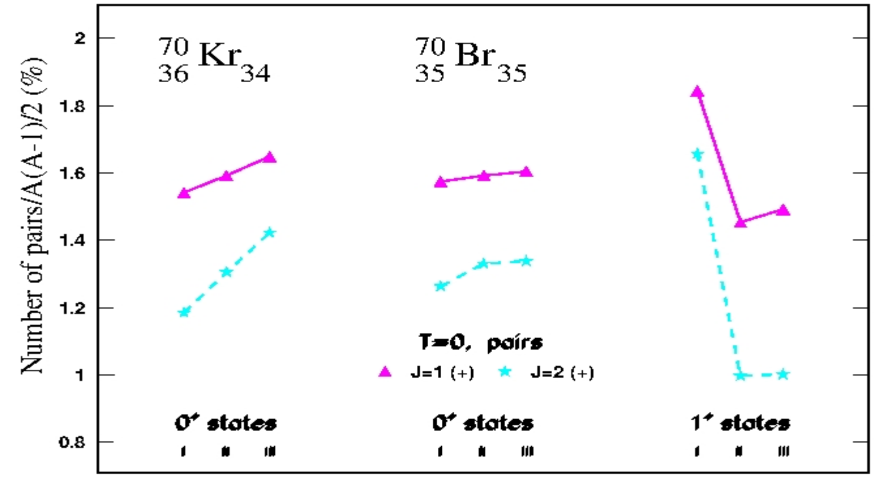

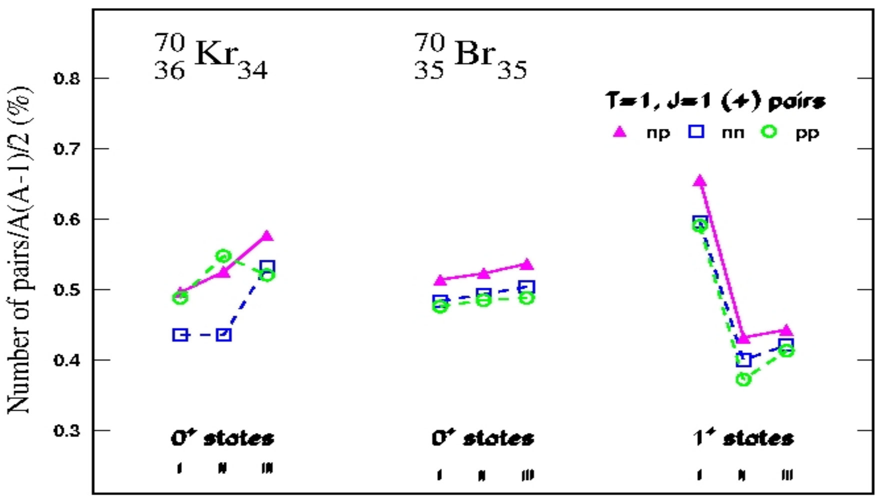

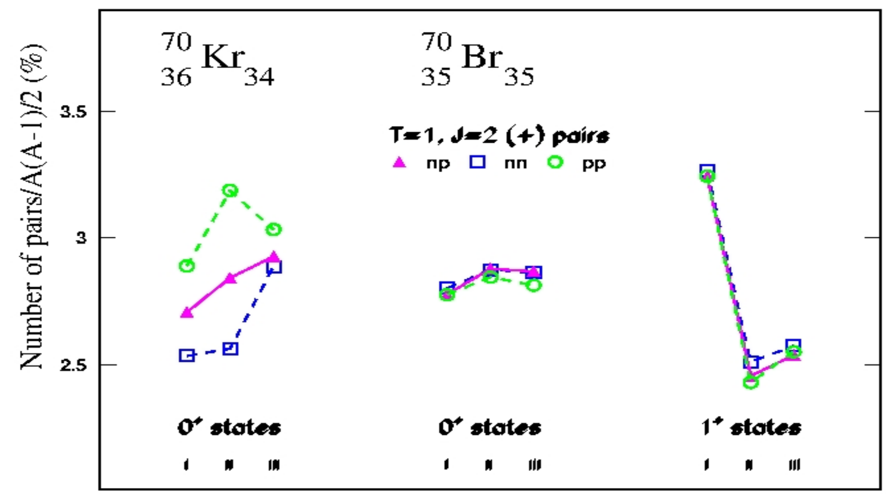

No enhancement of proton-neutron T=0 pairing correlations for GT contributing low-lying 1+ states

(preliminary results)

Triple shape coexistence and shape evolution in the N=58 Sr and Zr isotopes

A. Petrovici, Phys. Rev. C85 (2012) 034337

Neutron-rich Sr and Zr isotopes: - *rapid transition from spherical to deformed shapes*
- *sudden onset of quadrupole deformation for N > 58*

Positive parity states up to spin 20⁺ in ^{96}Sr and ^{98}Zr (12-dimensional *EXVAM many-nucleon bases*)

The amount of mixing for the lowest 0^+ states of ^{96}Sr.

$I[\hbar]$	spherical	prolate	oblate
0_1^+	36%	20%	44%
0_2^+	57%	18%	25%
0_3^+		69%	31%
0_4^+	4%	6%	90%

Particular case for 0⁺ states

- the lowest 0^+ VAMPIR configuration is spherical
- the 3-lowest 0^+ orthogonal EXVAM configurations (*s, o, p*) are situated in an energy interval of 375 keV

- maximum oblate-prolate mixing for 2^+ and 4^+ states

  $\Delta E\ (2^+_{oblate} - 2^+_{prolate}) = 24$ keV

  $\Delta E\ (4^+_{prolate} - 4^+_{oblate}) = 154$ keV

- spherical EXVAM configurations for spins 2^+ and 4^+ not found up to 4 MeV excitation energy

The mixing for the 2^+ and 4^+ states.

$I[\hbar]$	prolate	oblate
2_1^+	34(2)%	58(5)%
2_2^+	65%	33(2)%
4_1^+	56(1)%	36(6)%
4_2^+	43%	52(5)%

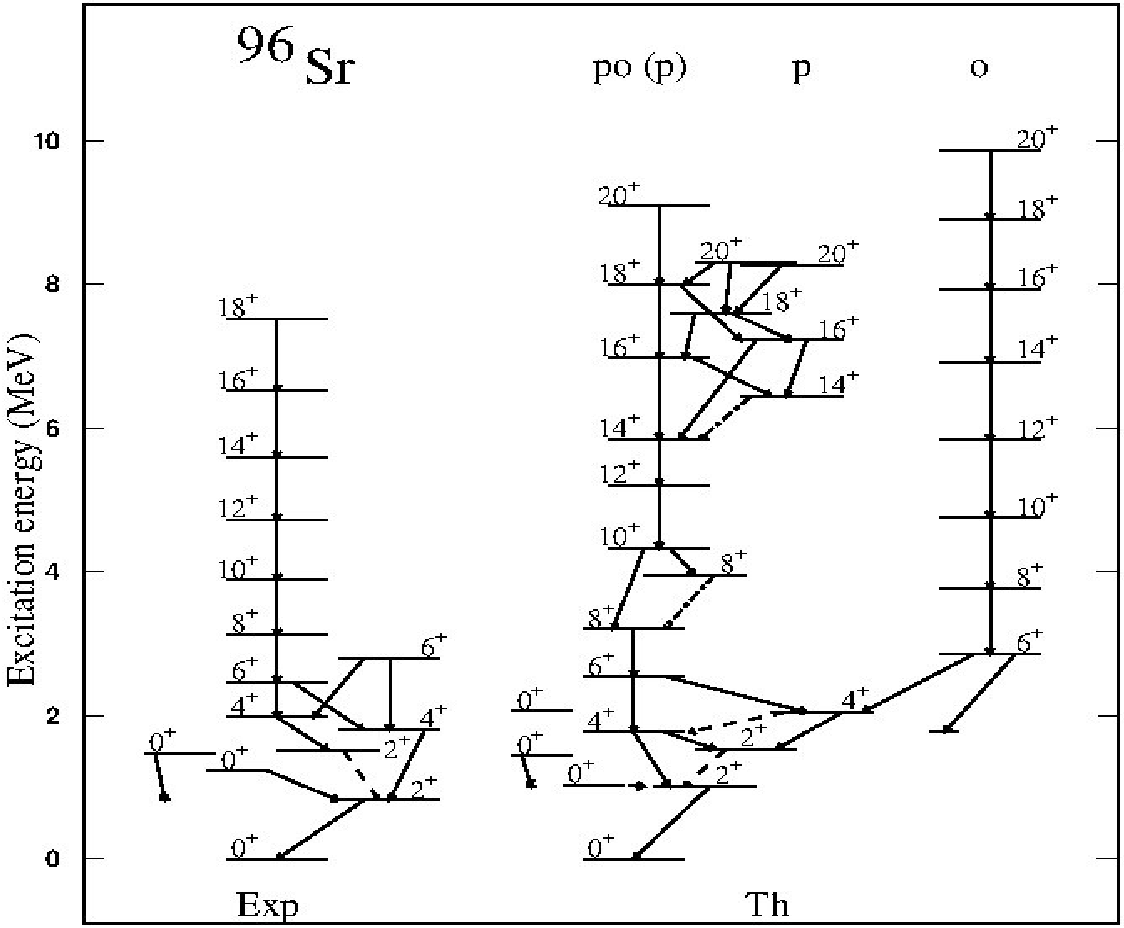

po(p)-band *- strong prolate-oblate mixing at low spins*

- variable prolate mixing at higher spins

almost pure o-band *feeds the second 4^+ (maximum o-p mixing)*

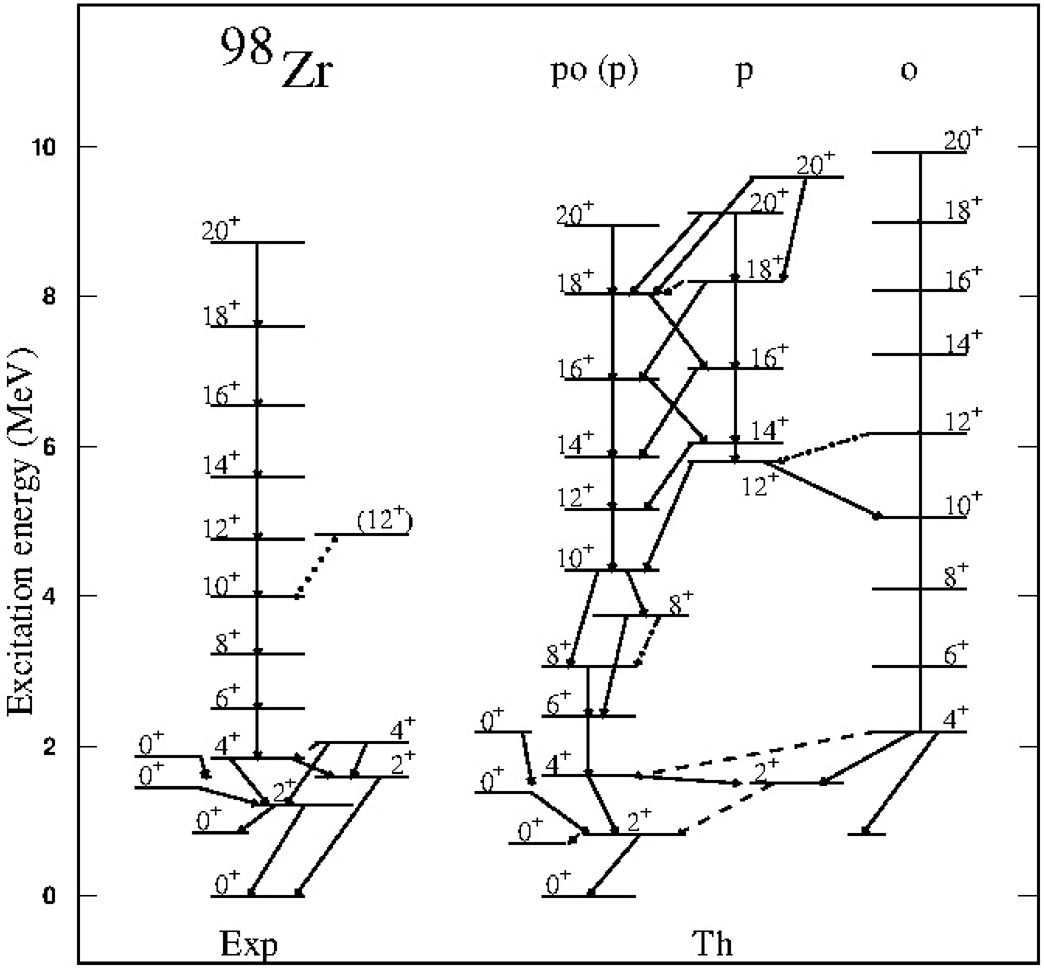

po(p)-band - *strong prolate-oblate mixing at low spins*
- *variable prolate mixing at higher spins*

o-band *feeds the second* 2^+ *(maximum o-p mixing)*

- the 3-lowest 0^+ EXVAM configurations (s, p, o) are separated by 323 keV

The amount of mixing for the lowest 0^+ states of ^{98}Zr.

$I[\hbar]$	spherical	prolate	oblate
0_1^+	12%	43%	45%
0_2^+	84%	12%	4%
0_3^+	1%	57%	42%
0_4^+	2%	10%	88%

- strong prolate-oblate mixing

$\Delta E\ (2^+_{prolate} - 2^+_{oblate}) = 206$ keV

$\Delta E\ (4^+_{prolate} - 4^+_{oblate}) = 431$ keV

The mixing for the 2^+ and 4^+ states.

$I[\hbar]$	prolate	oblate
2_1^+	60(8)%	31%
2_2^+	36%	63(1)%
4_1^+	83(7)%	10%
4_2^+	13(1)%	85(1)%

- spherical EXVAM configurations for spins 2^+ and 4^+ not found up to 4 MeV excitation energy

Occupation of valence single-particle orbitals for 0^+ states – sensitive to intrinsic deformation

$d^{\nu}_{5/2}$ occupation – essential for spherical 0^+ EXVAM configuration

$g^{\pi}_{9/2}$ occupation – significantly changing from intrinsically oblate to prolate deformed 0^+ EXVAM configurations

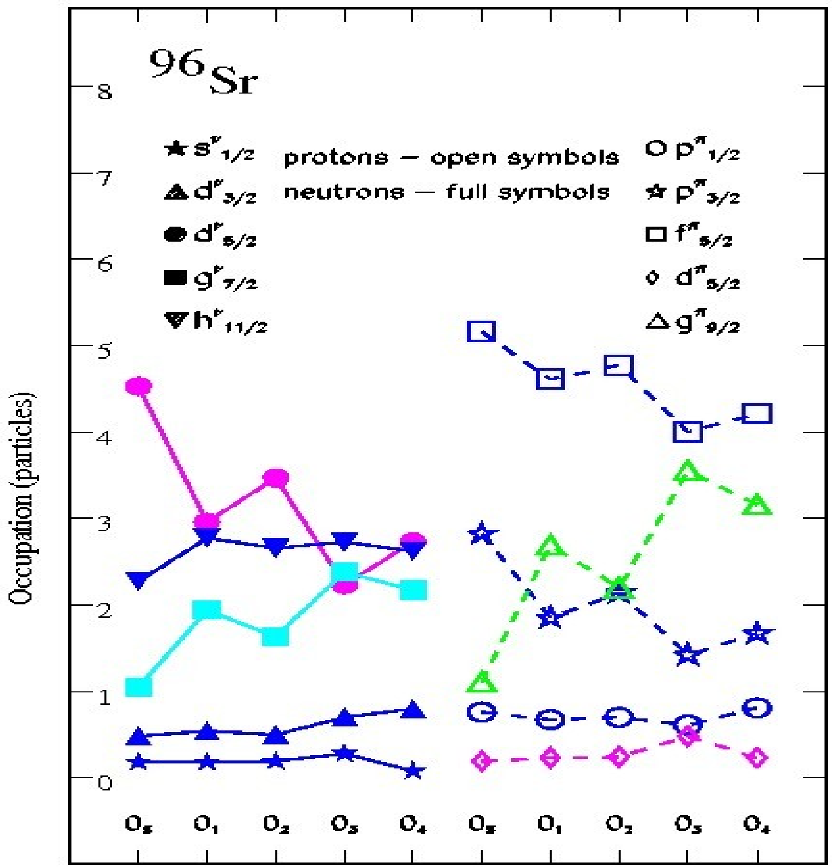

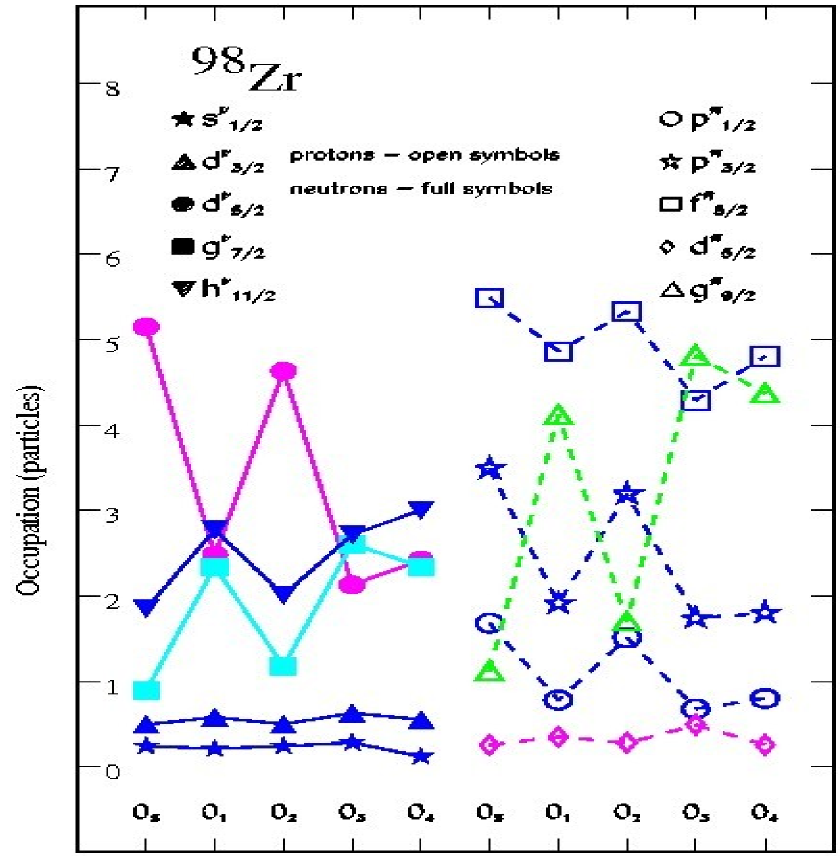

Strong E0 transitions support mixing of differently deformed configurations in 0^+ wave functions

$\rho^{2\,exp}_{max}(E0;0^+_3 \rightarrow 0^+_2) = 0.180$

$\rho^{2\,EXVAM}_{max}(E0;0^+_2 \rightarrow 0^+_1) = 0.066$

$\rho^{2exp}_{max}(E0;0^+_3 \rightarrow 0^+_2) = 0.075(8)$

$\rho^{2\,EXVAM}_{max}(E0;0^+_2 \rightarrow 0^+_1) = 0.060$

Evolution in structure with spin and excitation energy revealed by relevant spherical occupations

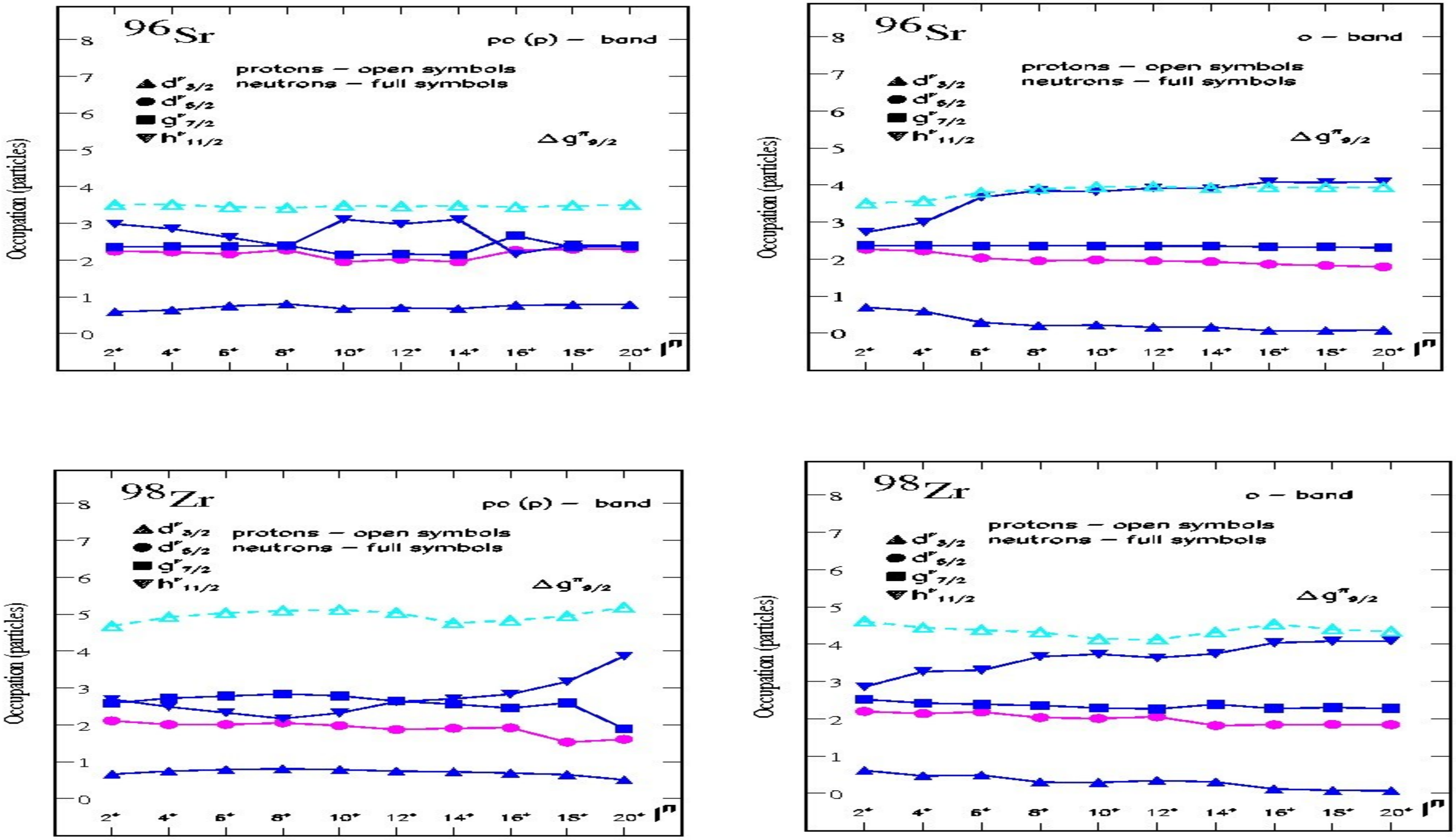

changes in structure corroborated with underlying shapes and evolution of shape mixing

Changes in structure revealed by angular momentum alignment and magnetic properties

dominant contribution from ν-$h_{11/2}$ and π-$g_{9/2}$ alignment

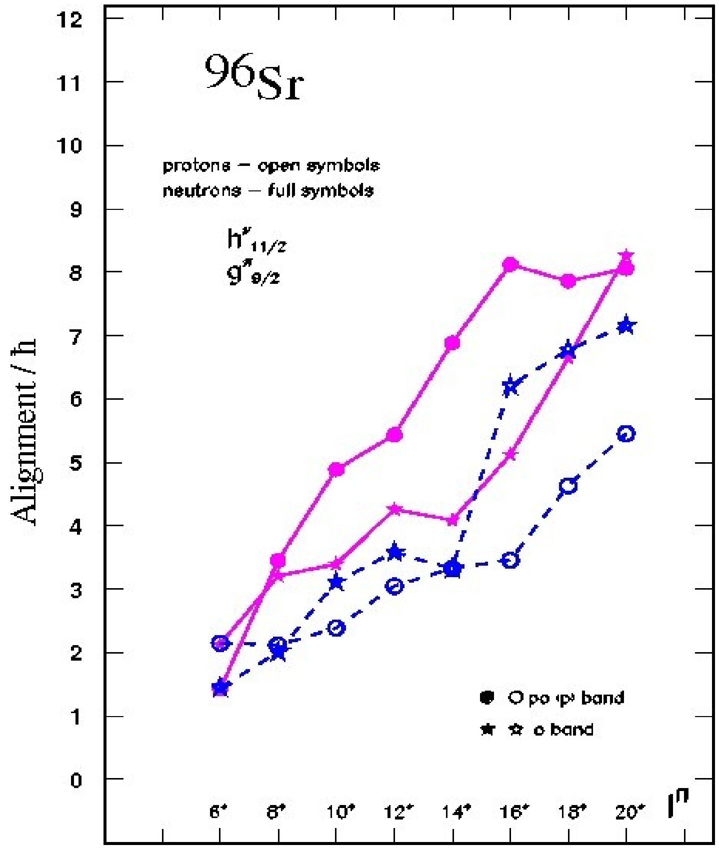

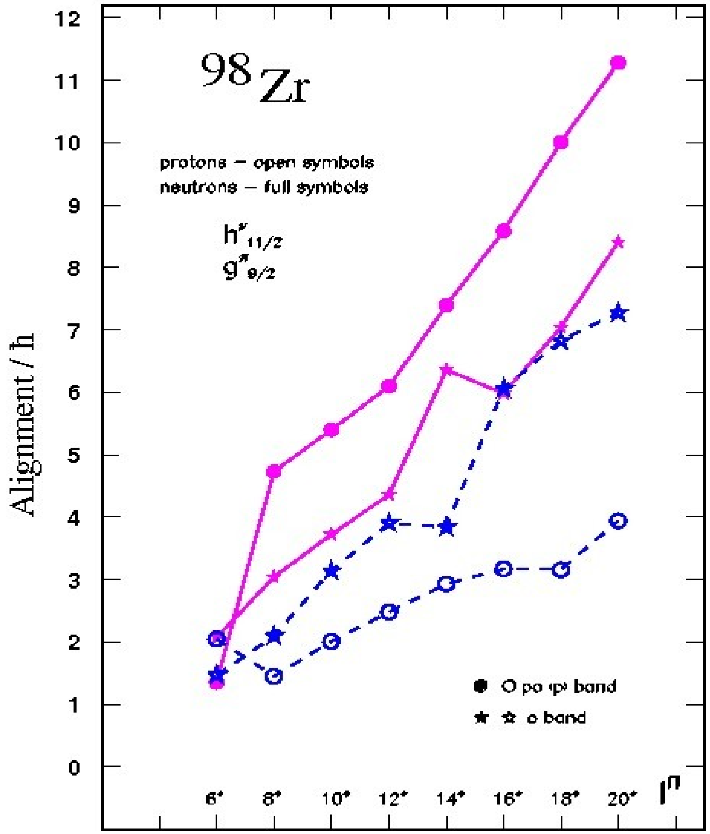

• *g-factor :* ≅ 0.24 ($I^{\pi} \geq 8^+$) (po(p)-band)
* *g-factor :* ≅ 0.50 ($I^{\pi} \geq 10^+$) (o-band)

• *g-factor :* ≅ 0.14 ($I^{\pi} \geq 8^+$) (po(p)-band)
* *g-factor :* ≅ 0.44 ($I^{\pi} \geq 10^+$) (o-band)

$B(M1; 8^+_3 \rightarrow 8^+_1) = 1.29\ \mu^2_N$

$B(M1; 8^+_2 \rightarrow 8^+_1) = 1.60\ \mu^2_N$

B(E2;ΔI = 2) strengths → fragmentation ↔ mixing

$B(E2; I \rightarrow I-2)$ values (in $e^2 fm^4$) for the lowest bands of ^{96}Sr (EXVAM) (effective charges $e_p = 1.3$, $e_n = 0.3$).

$I[\hbar]$	$po(p)$-band	o-band
2^+	795 340(209) (old) 580 (preliminary-Isolde)	
4^+	1770 (187)	1901 (12)
6^+	1911 (560)	1484 (215) (89)
8^+	2127 (361)(122)	1436 (159) (121) (99)
10^+	819 (1329) (168)	1514 (231)
12^+	2332 (142)	1760
14^+	2354 (57) (44)	1392
16^+	238 (2237) (160)	1590
18^+	753 (1374) (248)	1459
20^+	2183 (97)	1359

$B(E2; I \rightarrow I-2)$ values (in $e^2 fm^4$) for the lowest bands of ^{98}Zr (EXVAM) (effective charges $e_p = 1.3$, $e_n = 0.3$) .

$I[\hbar]$	$po(p)$-band	p-band	o-band
2^+	1140 (198)(161)		1305 (28) (18) (15)
4^+	2072 (620)		1593 (56)
6^+	2558 (101)		1662
8^+	1802 (942)(153)		1572 (123)
10^+	719 (1430)		1314 (119) (100)
12^+	2300 (216)	731 (345) (212)	663 (621) (307)
14^+	2428 (123)	1840 (392)	1094 (494)
16^+	1360 (832) (190)	548 (246) (1421)	602 (250) (195)
18^+	863 (207) (1416)	1347 (713) (808)	1115
20^+	409 (1958)	347 (185) (1972)	1313

Experimental lifetimes for intermediate spin states: simultaneous fit to several levels suggests deformation

$Q^{exp}_0 (12^+ \rightarrow 10^+ \rightarrow 8^+) = 220\ (15)\ efm^2$

$Q^{exp}_0 (12^+ \rightarrow 10^+ \rightarrow 8^+ \rightarrow 6^+) = 200\ (10)\ efm^2$

Spectroscopic quadrupole moments → deformation and mixing

Q_2^{sp} (in efm^2) for the lowest bands of ^{96}Sr (effective charges $e_p = 1.3$, $e_n = 0.3$).

$I[\hbar]$	po(p)	o
2^+	9.5	***0 (preliminary-Isolde)***
4^+	-23.9	1.4
6^+	-100.3	75.5
8^+	-120.1	77.3
10^+	-120.7	94.4
12^+	-124.1	94.6
14^+	-124.5	90.5
16^+	-130.0	85.4
18^+	-126.2	80.1
20^+	-124.4	68.1

Q_2^{sp} (in efm^2) for the lowest bands of ^{98}Zr (effective charges $e_p = 1.3$, $e_n = 0.3$).

$I[\hbar]$	po(p)	p	o
2^+	-36.6		7.1
4^+	-89.6		54.7
6^+	-115.5		76.7
8^+	-126.7		70.7
10^+	-130.1		58.2
12^+	-129.1	-98.5	55.6
14^+	-126.1	-121.2	30.5
16^+	-126.6	-123.0	60.8
18^+	-124.2	-134.4	74.9
20^+	-125.6	-135.4	68.9

po(p)-band: β_2^{EXVAM} $(8^+/10^+/12^+) \cong$ **0.3**

o-band: β_2^{EXVAM} $(8^+/10^+/12^+) \cong$ **-0.19 ÷ -0.23**

o-band: β_2^{EXVAM} $(8^+/10^+/12^+) \cong$ **-0.17 ÷ -0.13**

Gamow-Teller β decay of ^{102}Tc and ^{104}Tc (reactor decay heat)

M.D. Jordan, A. Algora A. Petrovici et al., Phys. Rev. C87 (2013) 044318

$^{102}Tc_{59} \rightarrow {}^{102}Ru_{58}$

$Q_\beta = 4.532 \pm 0.009$ MeV

$1^+_{gs} \rightarrow 0^+ \ / \ 1^+ \ / 2^+$

$T_{1/2} = 5.28(15)$ s

$^{104}Tc_{61} \rightarrow {}^{104}Ru_{60}$

$Q_\beta = 5.516 \pm 0.006$ MeV

$3^+_{gs} \rightarrow 2^+ \ / \ 3^+ \ / 4^+$

$T_{1/2} = 1098(18)$ s

complex EXCITED VAMPIR wave functions

$1^+_{gs} \rightarrow$ 53% oblate / 47% prolate
(7 EXVAM components)

$3^+_{gs} \rightarrow$ > 99% prolate
(7 EXVAM components)

$^{102}Ru_{58}$

complex EXCITED VAMPIR bases:

26 orthogonal projected configurations

for the spins 0^+, 1^+, 2^+

Gamow-Teller contributing states

0^+ : from 85% to 26% prolate components
including almost spherical ones

2^+ : from 78% to 26% prolate components

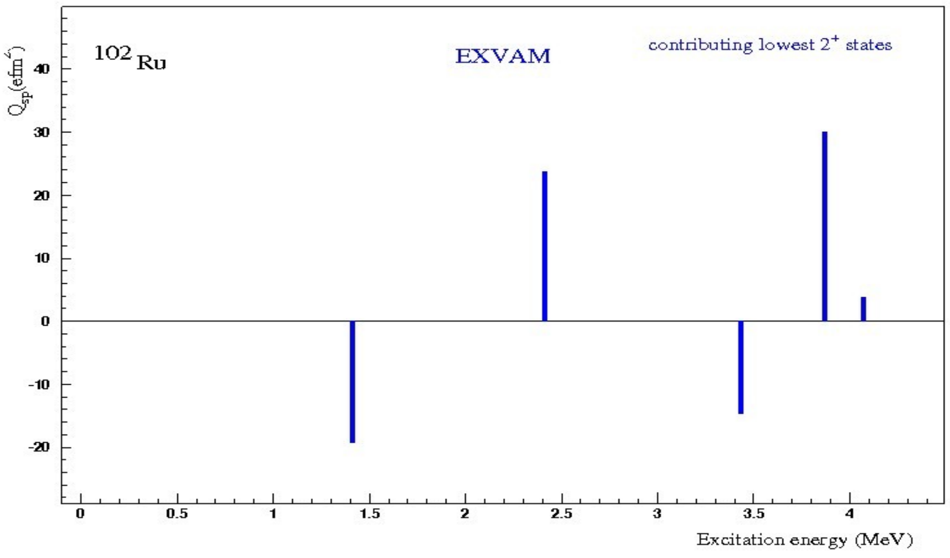

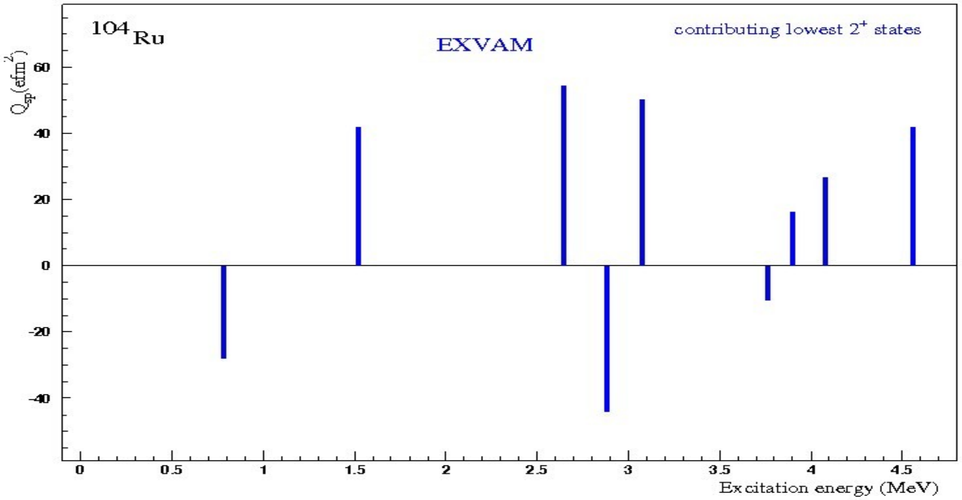

$^{104}Ru_{60}$

complex EXCITED VAMPIR bases:

25 orthogonal projected configurations

for the spins 2^+, 3^+, 4^+

Gamow-Teller contributing states

2^+ : from 82% to 9% prolate components

4^+ : from 96% to 8% prolate components

Spectroscopic quadrupole moments:

larger deformation for the N=60 states with respect to the N=58 ones

$^{102}Tc_{59} \rightarrow {}^{102}Ru_{58}$

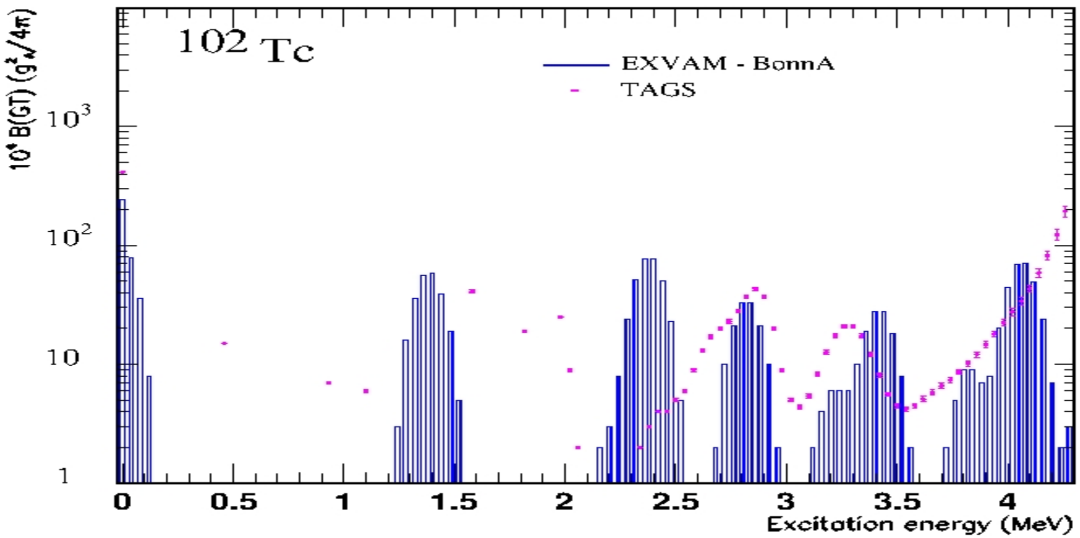

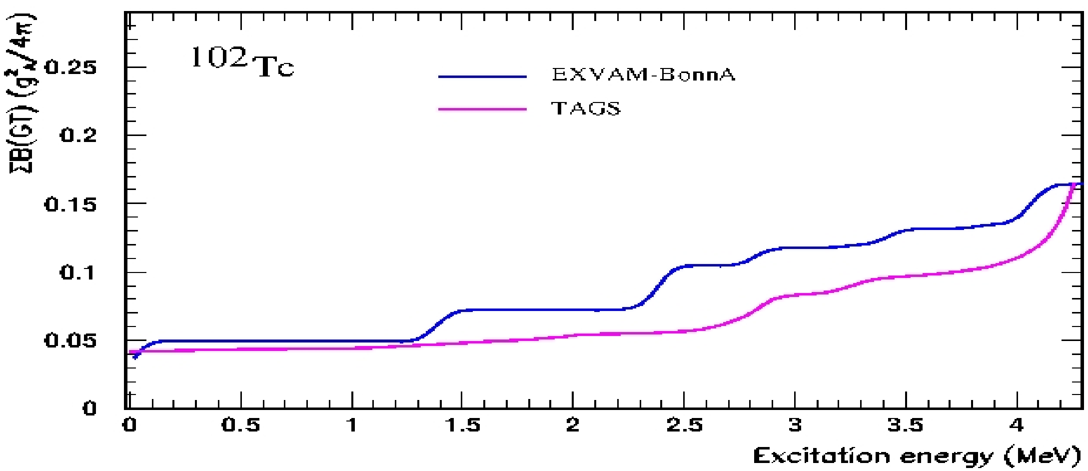

$T^{exp}_{1/2} = 5.3\ s$

$T^{EXVAM}_{1/2} = 6.6\ s$

Essential contribution from $g^{\pi}_{9/2} g^{\nu}_{7/2}$, $d^{\pi}_{5/2} d^{\nu}_{3/2}$, and $d^{\pi}_{5/2} d^{\nu}_{5/2}$ matrix elements

$^{104}Tc_{61} \rightarrow {}^{104}Ru_{60}$

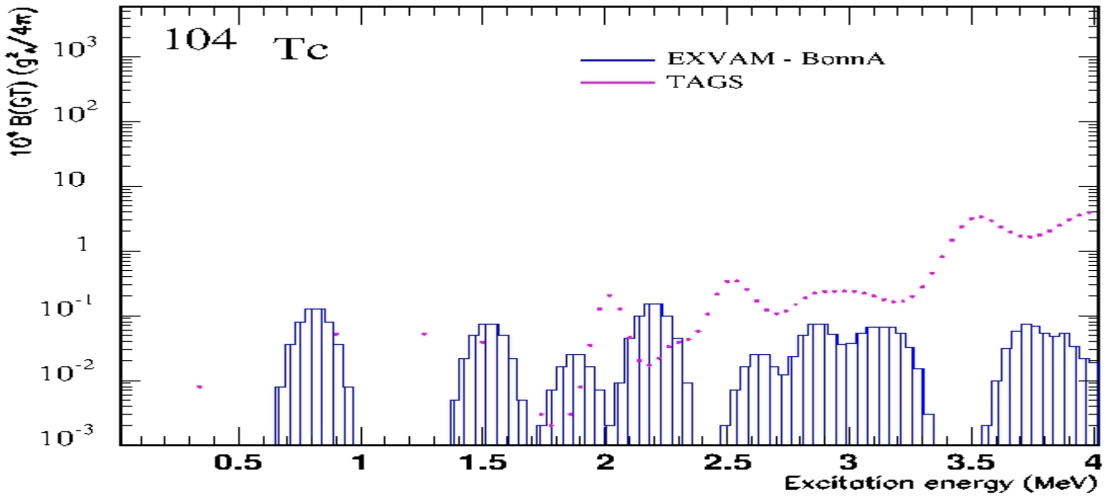

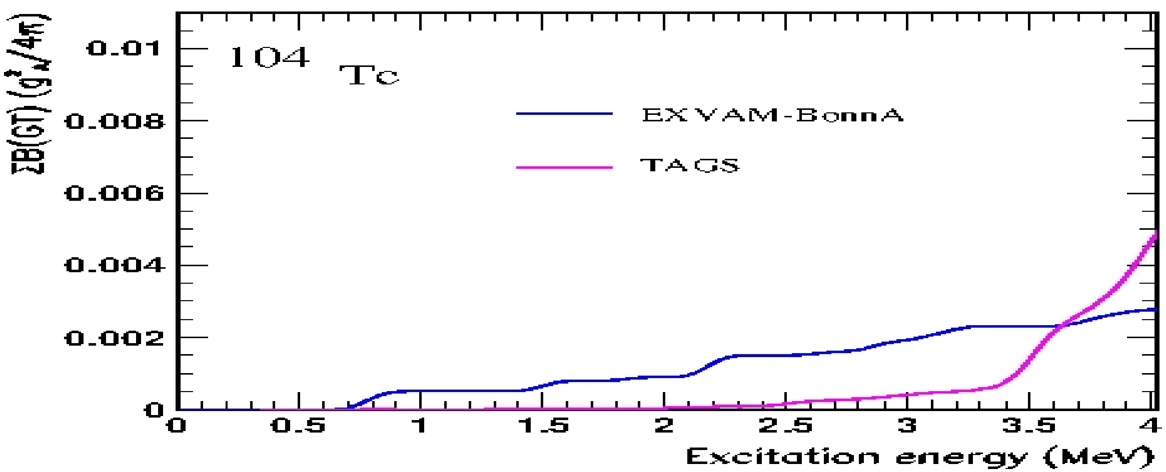

$T^{exp}_{1/2} = 1098$ s

$T^{EXVAM}_{1/2} = 385$ s

Contributions from $g^{\pi}_{9/2} g^{\nu}_{7/2}$, $d^{\pi}_{5/2} d^{\nu}_{3/2}$, $d^{\pi}_{5/2} d^{\nu}_{5/2}$, $p^{\pi}_{1/2} p^{\nu}_{3/2}$,, $p^{\pi}_{3/2} p^{\nu}_{1/2}$ matrix elements, all small, manifesting also cancellation effect

Gamow-Teller β-decay half-lives and β-delayed neutron emission probabilities of Zr isotopes relevant for the r-process

A = 104, 106

$^{98-110}$Zr chain : rapid transition from spherical to deformed shape
shape coexistence → competing prolate, oblate, and spherical shapes

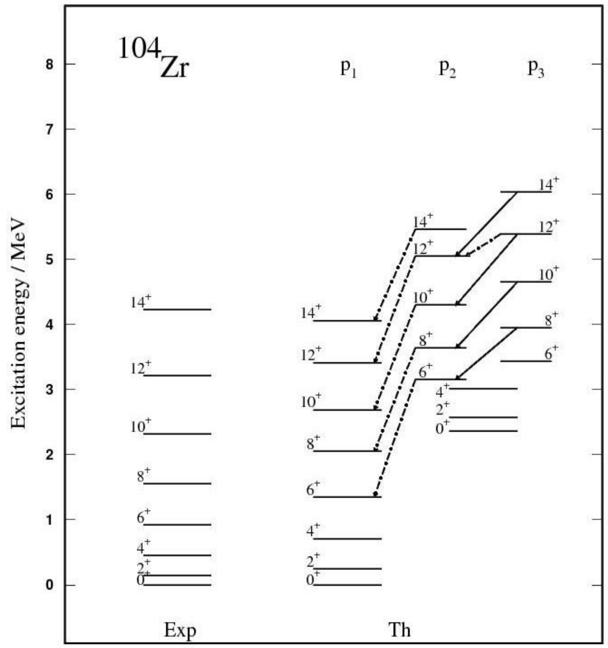

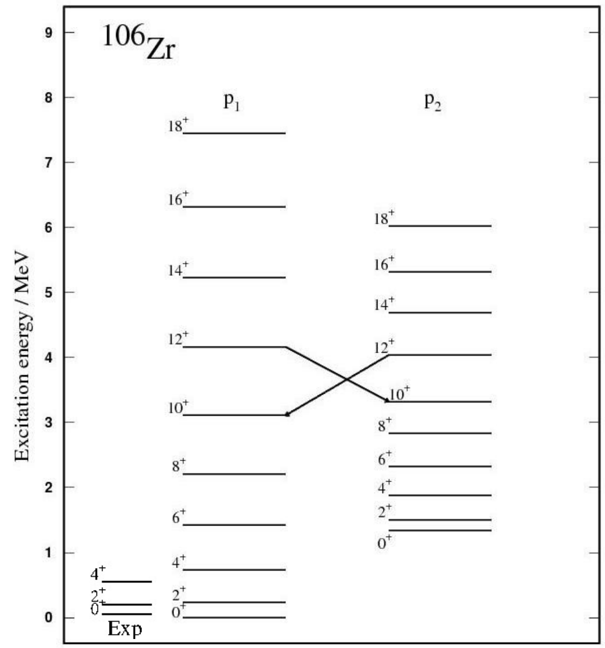

· *variable mixing of prolate deformed EXVAM configurations at intermediate and high spins*
· *ground state dominated (99%) by a strongly deformed EXVAM configuration*

A. Petrovici et al., J. Phys. 312 (2011) 092051

$^{104}Zr \rightarrow {}^{104}Nb$ $^{106}Zr \rightarrow {}^{106}Nb$ *NCSL-MSU / J. Pereira et al., Phys. Rev. C79 (2009) 035801*

A. Petrovici et al., Prog. Part. Nucl. Phys. 66 (2011) 287

complex* Excited Vampir many-nucleon basis: *50 projected 1^+ configurations in ^{104}Nb and ^{106}Nb

Gamow-Teller contributing states: large variety of spectroscopic quadrupole moments above 2 MeV excitation energy

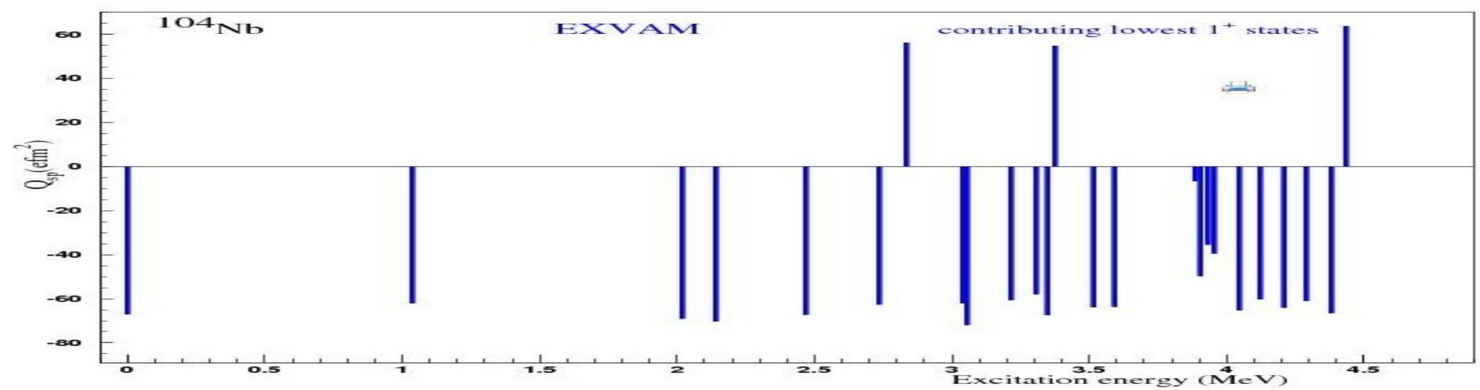

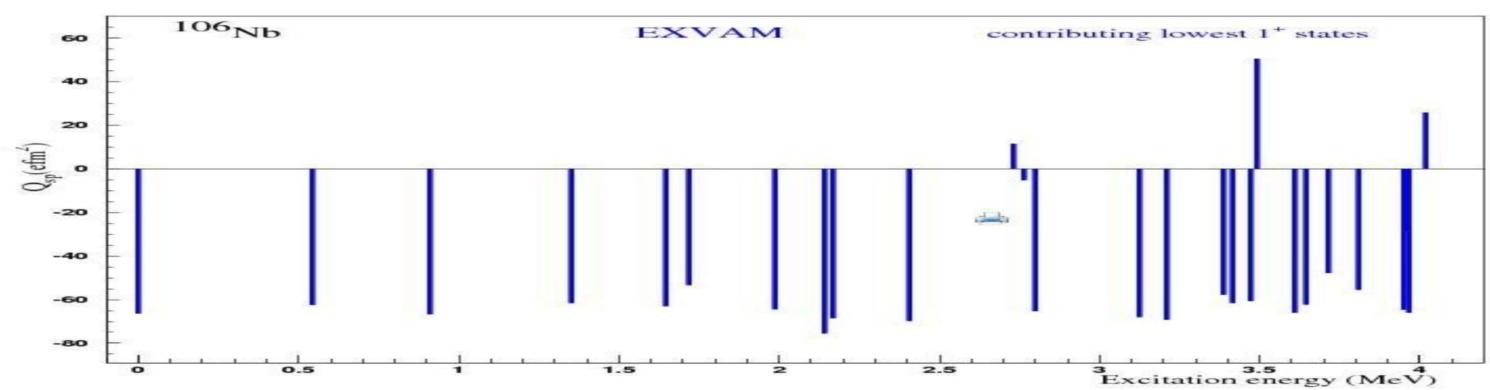

Gamow-Teller strength distribution specific for each isotope

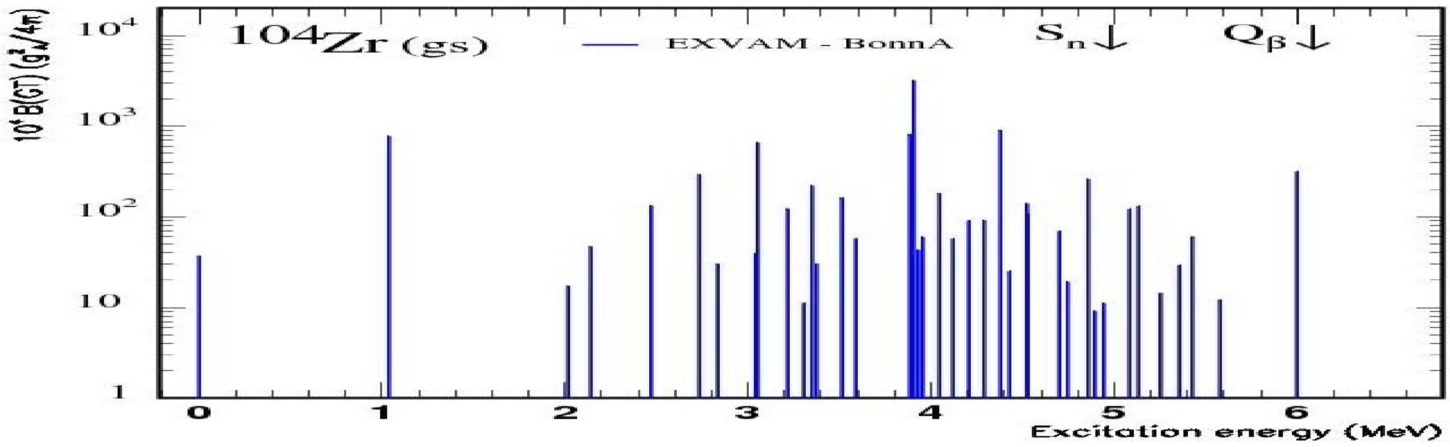

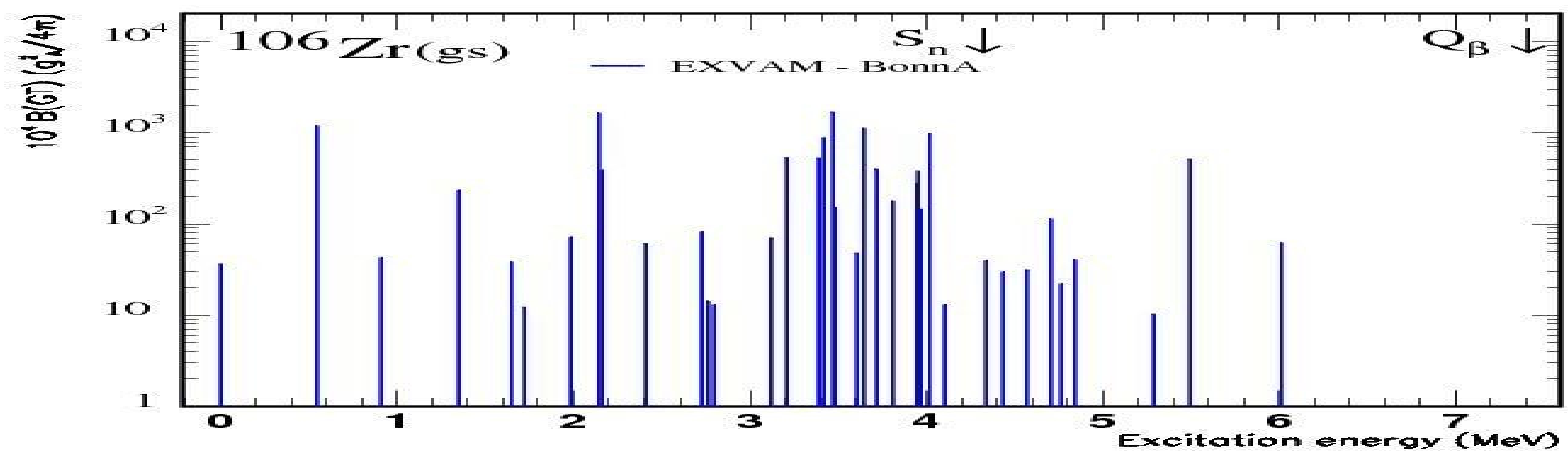

Essential contribution from $g^{\pi}_{9/2} g^{\nu}_{7/2}$, $d^{\pi}_{5/2} d^{\nu}_{3/2}$, *and* $d^{\pi}_{5/2} d^{\nu}_{5/2}$ *GT matrix elements*

Gamow-Teller accumulated strengths, half-lives, β-delayed ν-emission probabilities

$$P_n = \frac{\sum_{S_n}^{Q_\beta} f(Z, Q_\beta - E_{ex}) B(GT, E_{ex})}{\sum_{0}^{Q_\beta} f(Z, Q_\beta - E_{ex}) B(GT, E_{ex})}$$

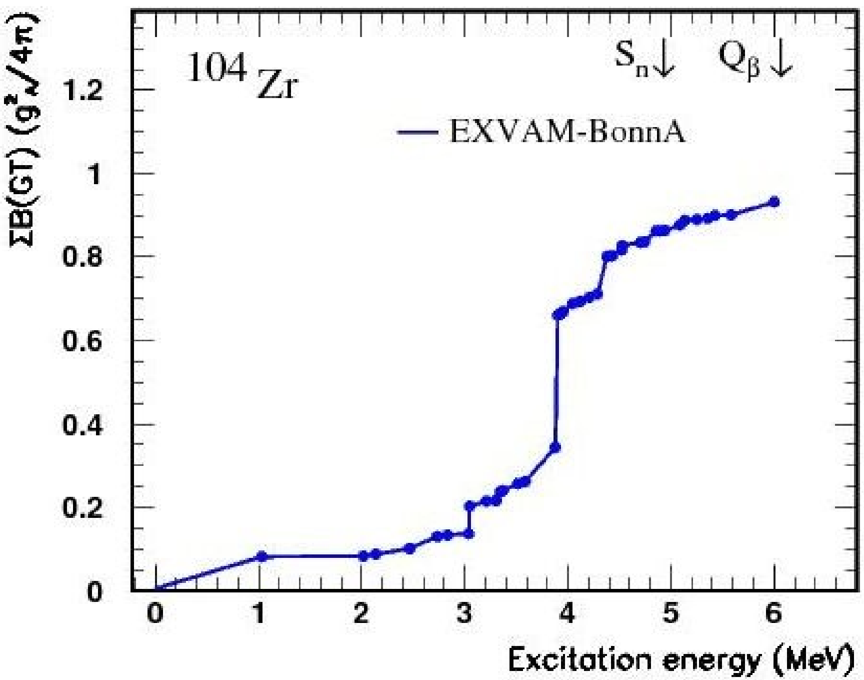

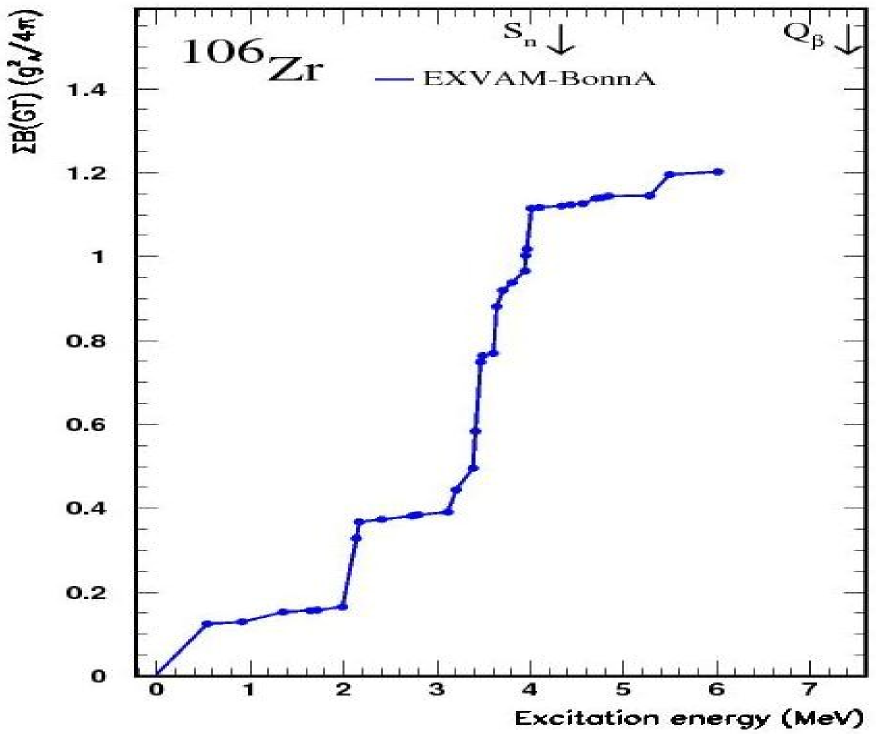

$T^{exp}_{1/2}$ 870(50)(30) ms (MSU 2009)
1200(300) ms (Mainz 1980)

$P^{exp}_n < 1$ % (MSU 2009)

$T^{EXVAM}_{1/2} = 2040$ ms
(50 1^+ states in ^{104}Nb)

$P^{EXVAM}_n \sim 1$ ‰

$T^{exp}_{1/2}$
260(20)(30) ms (MSU 2009)

$P^{exp}_n < 7$ % (MSU 2009)

$T^{EXVAM}_{1/2} = 230$ ms
(50 1+ states in ^{106}Nb)

$P^{EXVAM}_n \sim 2$ %

Summary and outlook

complex **EXCITED VAMPIR model** explains self-consistently

- **shape coexistence and isospin mixing effects on CED and *β*-decay of proton-rich A~70 nuclei**

- **experimental trends in neutron-rich A~100 isotopes :**

  - triple coexistence of spherical, prolate, oblate configurations in the structure of lowest 4 0^+ states

  - multifaceted yrast structure specific for ^{96}Sr and ^{98}Zr
  - remarcable difference in GT *β*-decay properties of ^{102}Tc and ^{104}Tc revealed by TAGS data

  - half-lives and β-delayed neutron emission probabilities of ^{104,106}Zr nuclei

The effective interaction is currently refined studying chains of proton-rich and neutron-rich nuclei

In collaboration with:

K. W. Schmid

Tuebingen University, Germany